Alzheimer Peptides Aggregate into Transient Nanoglobules That Nucleate Fibrils

Jinghui Luo,[†] Sebastian K. T. S. Wärmländer,[‡] Astrid Gräslund,*,[‡] and Jan Pieter Abrahams*,[†]

[†]Leiden Institute of Chemistry, Leiden University, Einsteinweg 55, 2333 CC Leiden, The Netherlands
[‡]Department of Biophysics and Biochemistry, Stockholm University, Svante Arrhenius väg 16C, SE-106 91 Stockholm, Sweden

S *Supporting Information*

ABSTRACT: Protein/peptide oligomerization, cross-β strand fibrillation, and amyloid deposition play a critical role in many diseases, but despite extensive biophysical characterization, the structural and dynamic details of oligomerization and fibrillation of amyloidic peptides/proteins remain to be fully clarified. Here, we simultaneously monitored the atomic, molecular, and mesoscopic states of aggregating Alzheimer's amyloid β (Aβ) peptides over time, using a slow aggregation protocol and a fast aggregation protocol, and determined the cytotoxicity of the intermediate states. We show that in the early stage of fast fibrillation (the lag phase) the Aβ peptides coalesced into apparently unstructured globules (15−200 nm in diameter), which slowly grew larger. Then a sharp transition occurred, characterized by the first appearance of single fibrillar structures of approximately ≥100 nm. These fibrils emerged from the globules. Simultaneously, an increase was observed for the cross-β strand conformation that is characteristic of the fibrils that constitute mature amyloid. The number and size of single fibrils rapidly increased. Eventually, the fibrils coalesced into mature amyloid. Samples from the early lag phase of slow fibrillation conditions were especially toxic to cells, and this toxicity sharply decreased when fibrils formed and matured into amyloid. Our results suggest that the formation of fibrils may protect cells by reducing the toxic structures that appear in the early lag phase of fibrillation.
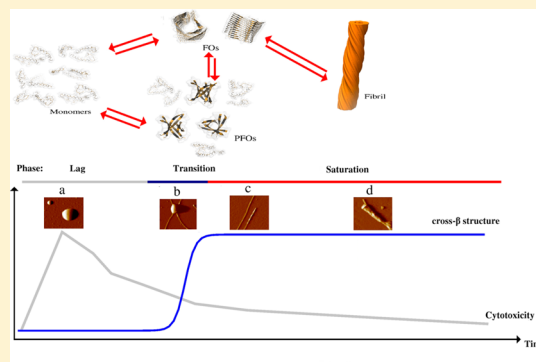
In many diseases, amyloidogenic proteins—including the Alzheimer's disease-related Aβ40 and Aβ42 peptides, but also the islet amyloid polypeptide, α-synuclein, prion protein, and insulin—assemble into disease-associated cross-β fibrils.[1−3] Before and/or during the formation of fibrils, the peptides or proteins refold into a β sheet structure. Prior to forming mature amyloid, monomeric peptides form aggregates of diverse morphologies, indicating complex aggregation pathways. For instance, fibrils of the human Aβ peptide can exist in several distinct and persistent structural variants, and preformed seeds determine the structural variant of the fibril.[4] Similar observations have been reported for prion proteins.[1]

Amyloid fibrillation includes a lag phase, a transition phase, and a saturation phase.[5,6] These stages also characterize crystallization, strongly suggesting that the formation of stable nuclei from which the fibrils grow is a rate-limiting step. During fibrillation, unfolded or partially unfolded proteins associate into small, soluble prefibrillar oligomers (PFOs) and fibrillar oligomers (FOs), which eventually develop into mature fibrils.[6−8] PFOs and FOs are morphologically and immunologically distinct, and specific antibodies can discriminate among PFOs, FOs, and annular protofibrils.[9] Importantly, PFOs have been shown to be more toxic than FOs (mass by mass).[10,11] FOs were reported to nucleate spontaneously from the monomeric state and are recognized by antifibril antibodies.

FOs may represent fibril nuclei or small pieces of fibril that grow into fibrils by capturing soluble monomers at their ends.[9]

It is not clear whether the growth of FOs requires the presence of PFOs or what role PFOs play in fibril formation. It has been proposed that PFOs are cylindrical β barrels, in contrast to the linear β sheets of the FOs. This theory is based on an analogy with the behavior of the αB crystallin chaperone protein, which can exist as aggregated amyloid or as a hexameric β barrel. In amyloid, the peptides interact through in-register hydrogen bonds, but in the barrel, the interstrand hydrogen bonds between the β strands are out of register. It was hypothesized that such barrel structures are similar to the more toxic structures of the Aβ peptide that precede amyloid formation,[10,11] but other data indicate that soluble early, toxic oligomers of the Aβ peptide do contain the cross-β structure.[21] Besides the structures mentioned above, many more intermediate complexes have been reported, and the nomenclature and understanding of all these intermediate complexes are still developing.[12]

There are many reports interpreting the secondary structure, toxicity, and morphologies of Aβ aggregates in specific phases of fibrillation. For instance, Dahlgren et al. reported that Aβ42

oligomers are 10 times more toxic to neuronal cells than fibrils (mass by mass) and even 40-fold more toxic than the unaggregated peptide.[13] Another study showed that Aβ40 first forms large aggregates that subsequently convert into small aggregates, although little information was provided about the structure of these aggregates.[14] We also investigated the structural transition and fibrillation of Aβ in the absence and presence of different ligands (such Gramicidin S,[15] poly-amines,[16,17] lysozyme,[18] and carbon nanotubes[19]), yet it remains difficult to unequivocally correlate the biochemical and biophysical properties of these Aβ aggregates to the various stages of amyloid fibrillation, because of the heterogeneity and instability of the Aβ structures.

The aim of this study was to simultaneously characterize the structure and function of the Aβ peptide, as its aggregation state evolved through the lag, transition, and saturation phases. We aimed to correlate the following structural transitions and functional properties throughout the aggregation process, using the following techniques: the transition of secondary structure toward β sheet [circular dichroism (CD) spectroscopy], the evolution of the cross-β structure [thioflavin T (ThT) assay], the appearance of the aggregates [atomic force microscopy (AFM)], the changes in chemical shift [solution nuclear magnetic resonance (NMR)], and the biological activity using a cell toxicity assay.

As far as possible, we performed these assays simultaneously on the same sample. In Alzheimer's disease, Aβ aggregates at 37 °C; however, an NMR spectrum requires 1 h of measuring time at elevated concentrations, and Aβ aggregates into insoluble fibrils immediately under these conditions at 37 °C. We solved this problem by using two distinct aggregation protocols: a slow aggregation protocol at 20 °C with a high peptide concentration (for the NMR and cytoxicity assays) and a fast aggregation protocol with a lower peptide concentration and a physiological temperature of 37 °C (for AFM). To correlate the results obtained from these different aggregation protocols, we measured secondary structure transitions and cross-β formation using CD and ThT assays in both protocols.

■ **EXPERIMENTAL PROCEDURES**

Preparation of the Aβ(1−40) Peptide. Recombinant amyloid β peptides Aβ(1−40) and Aβ(1−42) were purchased either unlabeled or ^{15}N-labeled from AlexoTech AB (Umeå, Sweden) and prepared according to previously described protocols.[16]

Fast aggregation conditions were employed for CD spectroscopy, ThT fluorescence, and AFM.

A 10 mM ThT stock solution was prepared in dH$_2$O. This ThT stock was added in the required amounts to aliquots of finally freshly prepared Aβ(1−40) peptide, yielding final samples containing (in 2 mL) 5 μM ThT, 10 μM Aβ(1−40), and 10 mM phosphate buffer (pH 7.2). The 2 mL sample was pipetted into a 10 mm × 10 mm path length quartz cuvette with a plastic cap.

The sample was incubated at 37 °C and stirred with a 0.7 cm mechanical magnet at 22 rotations per second (1320 rpm) in a 1 cm cuvette. The measurements were taken in a Jobin Yvon Horiba (Longjumeau, France) Fluorolog 3 instrument. The excitation and emission wavelengths were 446 and 490 nm, respectively. The excitation and emission slits were set at 2 and 1 nm, respectively. The fluorescence data were obtained within time intervals of 5 s and fit to calculate the lag time and transition time using a Boltzmann function. During fluores-

cence measurement, the cuvette was temporarily and quickly transferred to a CD spectrometer (a Chirascan CD unit from Applied Photophysics, Surrey, U.K.). Far-UV CD spectra were recorded at 37 °C, between 190 and 260 nm using a bandwidth of 1.0 nm. Immediately after the CD measurements, the cuvette was returned to the Fluorolog instrument to continue the ThT fluorescence assay, ensuring the orientation of the cuvette was always the same.

After each CD measurement, 10 μL of sample (initial total volume of 2 mL) was quickly transferred from the cuvette and deposited on freshly cleaved mica for 3 min for AFM measurement. After 3 min, excess liquid on the mica was shaken off, and the mica plate with the deposited sample was rinsed once with 10 mM phosphate buffer (pH 7.2) and dried in a stream of dry air at room temperature. Specimens were mounted on a Multi-Mode atomic force microscope (Digital Instruments Nanoscope III), and images were collected in tapping mode at 70 kHz. The imaging was conducted in air, using silicon cantilevers with an asymmetric tip and a force constant of 3 N/m.

Slow aggregation conditions were used for CD spectroscopy, ThT fluorescence, solution NMR spectroscopy, and cell toxicity.

A Bruker Avance 700 MHz spectrometer with a cryogenic probe was used to record [1]H−^{15}N HSQC spectra at 5 °C of 500 μL of 90 μM ^{15}N-labeled Aβ(1−40) peptide [freshly prepared in 20 mM sodium phosphate (pH 7.2)] with 45 μM ThT at a 90/10 H$_2$O/D$_2$O ratio. Afterward, the sample was taken out and incubated in an Eppendorf tube for 0.5 h at 20 °C and put back into the NMR tube to record the next NMR spectrum. The same procedure and conditions were repeated after 1.7, 3.2, and 5.7 h. The data were analyzed using Sparky (http://www.cgl.ucsf.edu/home/sparky/). After each incubation, 10 μL of the sample was quickly transferred from the Eppendorf tube into 90 μL of 20 mM sodium phosphate buffer (pH 7.2) for CD and ThT fluorescence assays in a 0.5 mm × 10 mm cuvette (see above). Separately, a sample identical to that used for the NMR experiments [500 μL of 90 μM Aβ peptide with 45 μM ThT in 20 mM sodium phosphate (pH 7.2)] was used for cell toxicity assays.

Neuroblastoma SH-SY5Y cells with a maximal passage number of 15 were used. Cells were cultured to a confluency of 85% in a 75 cm^2 flask (Greiner Bio-one, catalog no. 658170), in Dulbecco's modified Eagle's medium (DMEM) (a 1:1 mixture of DMEM and Ham's F12 medium) and 10% supplemental fetal bovine serum, containing 1% (v/v) penicillin/streptomycin at 37 °C and 5% CO$_2$. Cells were detached with a 5 mM EDTA/PBS mixture for 5 min at 37 °C. Then cells were resuspended at a concentration of 200000 cells/mL in DMEM/F12 containing 1% (v/v) penicillin/streptomycin. The resuspended cells were plated at a volume of 50 μL and a cell density of 20000 cells/well in a 96-well plate. The plated cells were incubated for 48 h at 37 °C ans 5% CO$_2$. A sample with an identical Aβ40 peptide and buffer for the NMR, ThT, and CD measurements was prepared as described in the previous paragraph, and aliquots were taken after incubation at 20 °C for 0, 1.7, 3.2, 5.7, and 21 h, just like in the NMR, CD, and ThT analyses described above. The Aβ aggregates were diluted to a final concentration of 25 μM when they were added to the cell cultures. As a control, 20 mM sodium phosphate buffer was added at a volume of 50 μL in medium to each well and incubated for 48 h. After 48 h, the plate was equilibrated at room temperature for approximately
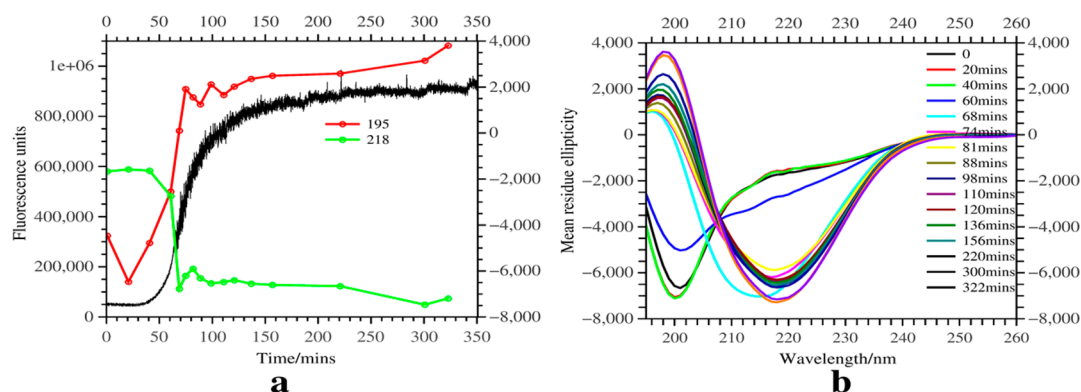
Figure 1. Synchronous measurements of Aβ40 fibrillation by (a) ThT fluorescence (black curve) and (b) CD spectroscopy. The transition of the secondary structure of Aβ40 was measured in parallel on the same sample and within the same cuvette using two independent assays. Note the slow conversion from random to β strand during the first 50 min, around an isodichroic point at 208 nm in the CD spectrum, followed by a rapid transition between 50 and 80 min. The CD intensities at 195 and 218 nm plotted vs time are plotted in panel a in red and green, respectively.

30 min. CellTiter-Glo Luminescent Cell Viability Assay (Promega, catalog no. G7571) compound was added to each well, and the plates were agitated on an orbital shaker for 2 min to induce cell lysis. The luminescence intensity was measured on a 384-well plate reader (Infinite M1000 PRO microplate reader) with an integration time of 1000 ms. Data were measured in three independent experiments, and statistical analysis was used to calculate the reported average values and standard deviations.

■ RESULTS

Fast Aggregation. We followed the kinetics of formation of the Aβ40 peptide cross-β structures that characterize amyloid fibrils using a ThT assay. The sample was incubated at 37 °C and stirred at 1320 rpm in a 1 cm cuvette. The resulting shear force is able to substantially promote the aggregation of Aβ peptide, compared to quiescent incubation. We observed a lag time of 50 min during which no cross-β structures were formed, which was followed by an exponential increase in fluorescence for ∼20 min (indicating cross-β amyloid fibrils were being formed rapidly) and a linear phase that lasted ∼20 min. Thus, the transition phase lasted around 40 min, and after ∼200 min, a steady state was reached (Figure 1). A similar, albeit faster, behavior was observed for the related Aβ42 peptide (see Figure S2 of the Supporting Information). These kinetic ThT results follow the typical pattern for Aβ aggregation and were confirmed by simultaneous CD spectroscopy of the same sample (measured in the same cuvette). The CD spectra are generally characterized by a transition from random coil to β sheet structure, with an isodichroic point around 208 nm. The CD spectra after 64 and 71 min are off the isodichroic point. Light scattering due to the presence of large aggregates can cause such an offset. The transition from random coil to β sheet is slow at first and accelerates after ∼50 min (Figure 1b). This time point coincides with the end of the lag phase we observed in the ThT assay. This rapid shift indicates that fibrils can grow quickly once the fibril nuclei have formed. Apparently, the transition from random coil to β sheet is catalyzed by the presence of fibril nuclei. For the Aβ42 peptide, the formation of fibril nuclei apparently is much more favorable, resulting in the more rapid formation of fibrils (Figure S2 of the Supporting Information).

ThT intercalates between the β strands in the fibril,[20] but there is no indication that it binds β barrels. CD spectroscopy has a similar signal for both cross-β structure and β barrels. The kinetics of the CD spectra and the ThT assay are very similar (compare the black curve with the red and green curves in Figure 1a). This indicates that the vast majority of β sheet that was being formed was incorporated into cross-β structures. It also indicates that if any β structure is formed during the lag phase (cross-β structure or β barrel) this can be only a small amount.

However, even if there was little indication of changes in secondary structure during the lag phase, AFM showed that during the lag phase, small, special aggregates were formed, which we term nanoglobules. These nanoglobules grew or coalesced over time (Figure 2) in a process that may compare well to classical phase separation, but on a much smaller scale. These spheres can explain why CD spectra during the transition phase deviate from the isodichroic point (the large spheres induce light scattering). After ∼60 min, fibrils started growing from the larger globular aggregates and continued to grow. Close inspection of the AFM images revealed that fibrils (some indicated by arrows in Figure 2) frequently lie over the, otherwise featureless, globular aggregates. In a significant number of cases, we observed that the fibrils emerged from both sides of the globules (see, for instance, Figure 2d), strongly suggesting that the fibrils can grow at both of their free ends and hence can accrue peptides from the solution. However, we cannot entirely exclude the possibility that fibers might also grow by directly incorporating peptides from the nanoglobules. After 340 min, well into the plateau observed using the ThT assay, the spheres were no longer visible and only fibrillar aggregates could be seen.

Slow Aggregation. For the NMR studies, Aβ aggregation had to be slowed by incubation at room temperature instead of 37 °C between the NMR measurements, which were taken at 5 °C to retain the peptide stability during the NMR measurement.[22,23] We ascertained by CD and ThT measurements that reducing the temperature slowed aggregation by a factor of ∼4 (compare Figures 1 and 3d,e). In parallel, we verified the aggregation state of the same batch of the Aβ peptide with a ThT assay (Figure S3 of the Supporting Information). The observed NMR signal is expected to mainly originate from the Aβ monomer and possibly from low-molecular weight aggregates. Because no significant chemical shift changes were observed, the results suggest that the soluble Aβ monomers
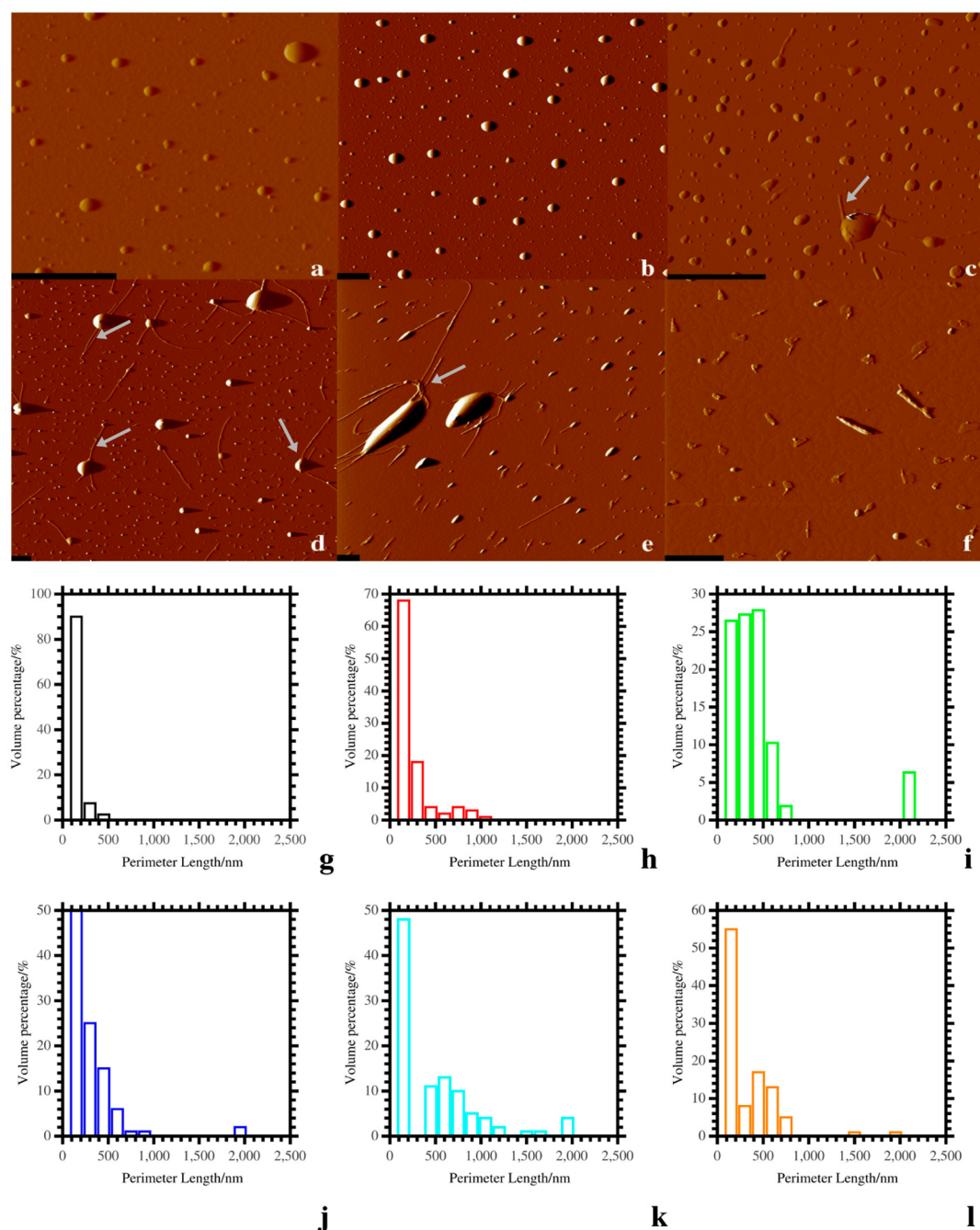
Figure 2. Aβ40 fibrillation observed by an atomic force microscope of the samples that were simultaneously studied by ThT fluorescence (Figure 1a) and CD spectroscopy (Figure 1b). (a−f) AFM images of Aβ40 from the different phases of fibrillation as monitored by a ThT fluorescence assay (Figure 1a). Aβ40 samples from the cuvette of the fluorescence assay were taken after (a) 20, (b) 40, (c) 57, (d) 71, (e) 91, and (f) 340 min for AFM measurements. The size of black scale bars is 1 μm. (g−l) Size distributions as defined by the ratio between the perimeter length distribution and the volume of aggregates corresponding to the AFM measurements at the given time points (a−f, respectively).

largely retain their initial random coil structure, at least during the lag phase.

However, there were changes in the intensity of the NMR signals of Aβ40 during the early lag phase (Figure 3 and Figure S4 of the Supporting Information). An overall reduction in Aβ amide HSQC cross-peak intensity was observed as the incubation progressed (Figure 3a−c). This loss of signal is probably caused by the aggregation of peptides into the small globular aggregates that we observed by AFM in the early lag phase in the "fast aggregation" protocol (Figure 2). We assume the monomers are in exchange with the aggregates on a slow or intermediate time scale.[24] After 30 min, ∼25% of the original cross-peak intensity remained, whereas after 100 min, ∼40% of the initial signal intensity was observed. After 200 min, only 20% of the signal intensity remained. While the signal intensity is expected to decrease over time because of aggregation, the signal recovery after 100 min was reproducible and unexpected (Figure S5 of the Supporting Information). Here we speculate about a possible mechanism. The observed oscillatory behavior of the NMR signal during the lag phase may be caused by fusion of aggregates initially dominating over growth of the total mass of the globular aggregates. When globular aggregates
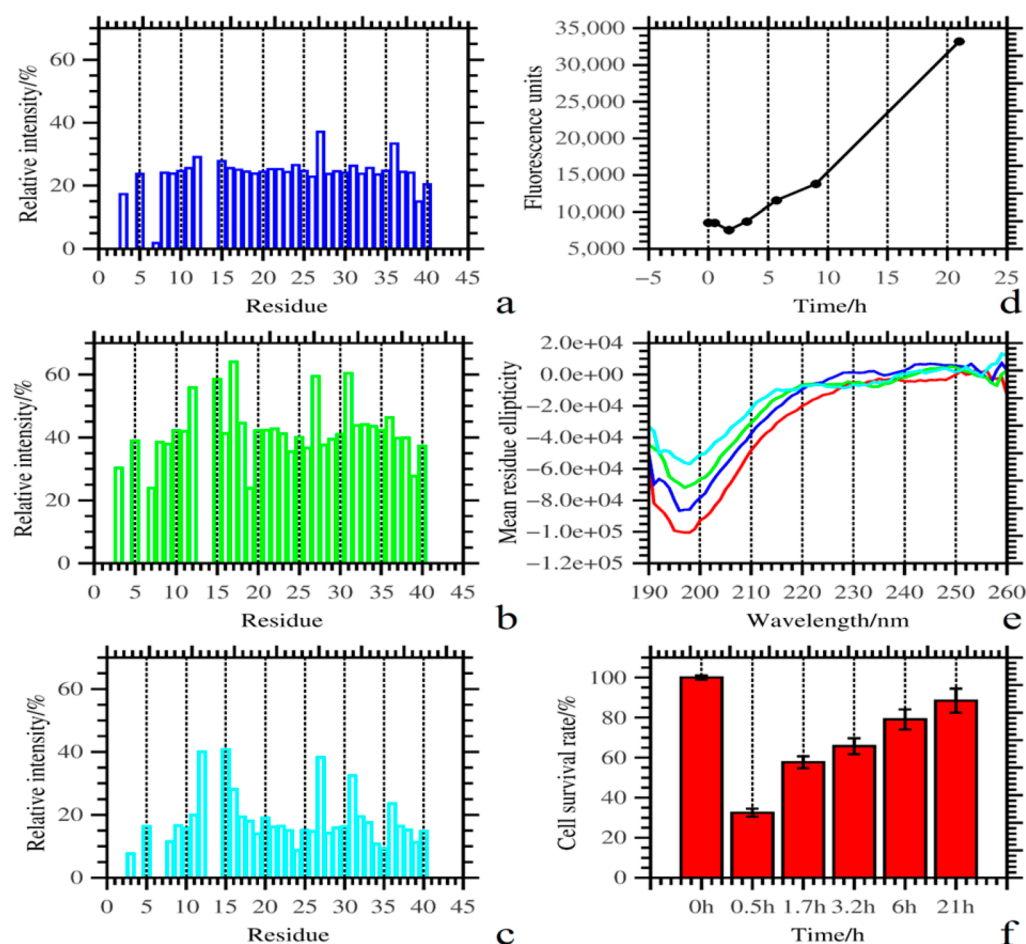
Figure 3. (a−c) Relative intensities of NMR cross-peaks of Aβ40 after incubation at 20 °C for 0.5, 1.7, and 3.2 h, respectively. (d) Appearance of cross-β structure formation within the NMR sample as measured by a ThT assay. (e) Changes in secondary structure of the NMR sample as measured by CD spectroscopy: spectra after incubationat 20 °C for 0 h (red), 0.5 h (blue), 1.7 h (green), and 3.2 h (cyan). (f) Cell toxicities of identical samples indicate that the most toxic species is formed early in the incubation and that over time the samples become less toxic.

fuse, the total surface area of the aggregates decreases, causing soluble monomers temporarily caught on the globule surface to be released, thus increasing the intensity of their NMR signal. When globular aggregates subsequently grow by net accretion of soluble peptides from solution, this reduces the intensity of their NMR signal.

To directly monitor the formation of larger globular aggregates, we performed size exclusion chromatography on Aβ40 aggregates prepared using the slow aggregation protocol (Figure S6a of the Supporting Information). We observed three main peaks (a−c). Comparison to size exclusion standards (Figure S6b of the Supporting Information) indicates that next to globules ∼100 kDa in size (peak a in Figure S6a of the Supporting Information), the sample also contains trimers and monomers (peaks b and c, respectively, of Figure S6a of the Supporting Information). The size of the large globular aggregates observed via size exclusion chromatography is a lower bound of the size of these globules in the NMR tube, as the globular complexes would have partially dissociated during chromatography.

One of the motivations of our studies was to relate conformational changes of the Aβ peptide to its toxicity. It is known that the early aggregates on a weight basis are more toxic than the mature fibrils; we used the "slow aggregation" protocol and performed aggregation of the Aβ peptide at 20 °C, just as in the NMR experiment. We took samples at the same

time points as in the NMR experiments and added them to growing neuroblastoma SH-SY5Y cells (Figure 3f). In parallel, we verified the aggregation state of the same batch of sample with a ThT assay (Figure S3 of the Supporting Information). We observed no effect on cell viability if the monomeric Aβ was added directly to the cells, without being allowed to start aggregating. However, 30 min into the lag phase, cell viability was severely affected, indicating that especially in the early stages of Aβ aggregation, the most toxic forms are produced. When aggregation was allowed to progress, cell viability increased again, indicating that the later-stage aggregates, in which fibrillar structures could be recognized via AFM, were less toxic or protected the cells.

■ DISCUSSION

To shed additional light on the aggregation process, we measured the conformational states of the peptides using a range of techniques and related these states to the development of nanoscopic structures of Aβ peptides, and in a separate assay, we determined their toxicity. Our results are summarized in Figure 4. Clearly, the peptides can be present in at least four different phases: (i) in solution, (ii) in a globular aggregate, (iii) in a fibril, and (iv) in amyloid. Our AFM data indicate that nanoglobular aggregates are formed very early in the aggregation process from the dissolved monomers and that
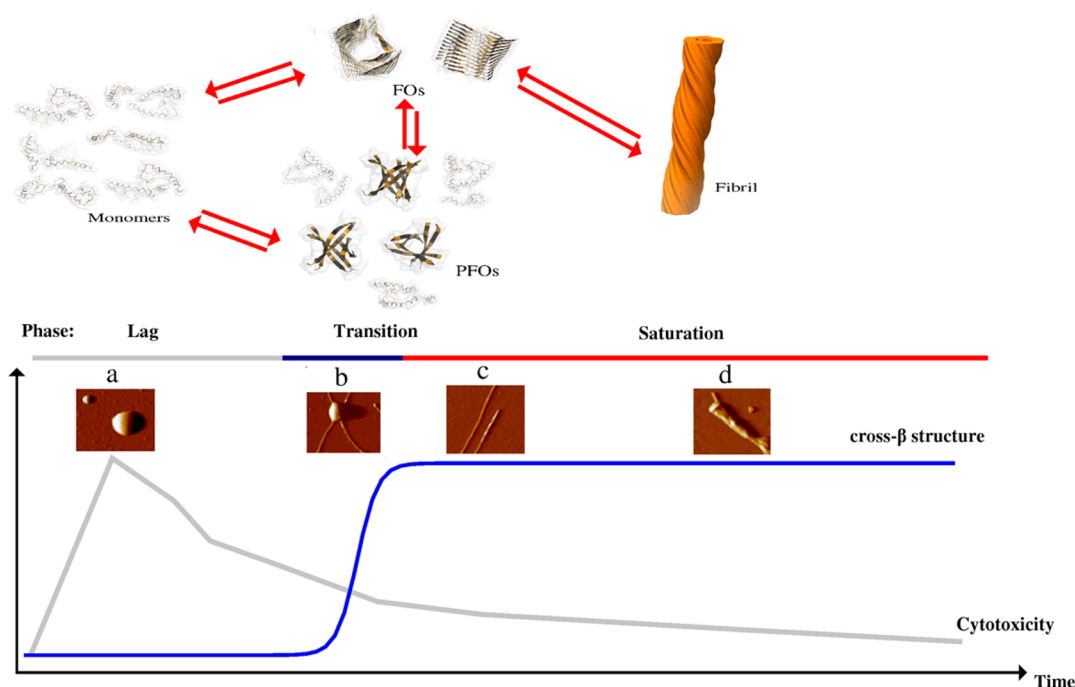
Figure 4. Summary of the changes to the secondary structure, cell toxicity, and morphology of Aβ oligomers as they pass through different phases of amyloid fibrillation. There are three different phases in amyloid fibrillation: lag, transition, and saturation phases. In the lag phase, the fibrillation pathway starts with a disordered monomer and can diverge in two directions to form aggregate variants that we also observed via AFM. The aggregates show a steep decrease in toxicity in the transition phase. When the amyloid β peptide passes from the lag phase to the saturation phase, its secondary structure is converted from random to β sheet during the transition phase.

these nanoglobules can coalesce into (much) larger ones and can nucleate fibrils. The appearance *in vitro* of similar spherical oligomers of Aβ40 that can, probably through conformational conversion, nucleate fibrils has been observed previously.[25−27] Also, the formation of prion and α-synuclein fibrils is associated with a similar conformational conversion mechanism.[28,29]

Extensive conversion of the random coil structure to β sheet conformation is not yet occurring during the early globule-forming stage, as our CD data indicate, although we cannot exclude the possibility that some β sheet could be forming. The observation of phase separation strongly suggests that the initial conformational change of the Aβ peptide results in the formation of a relatively more hydrophilic complex, which then separates from the solution to form the small globular aggregates. Whether conformational rearrangements, including initial complex formation, are taking place within the globular aggregates is difficult to assess, as these would be invisible to our NMR experiments. However, our AFM results suggest a (rare) nucleation event that takes place in or on the globular aggregates before fibrils can be nucleated. As we observe the fibrils to form more readily on large rather than small globular aggregates, we assume that fibril nucleation is a stochastic process: the larger the aggregate, the greater the chances of nucleation. However, we cannot exclude the possibility that different conformations, more effective in fiber nucleation, dominate in the larger aggregates, compared to the nano-globules. The emergence of the fibrous phase marks the start of the transition state. This stage is characterized by the conversion of peptides into a β strand conformation and the formation of cross-β sheets (as indicated by CD spectroscopy and ThT fluorescence, respectively). The fibrils bundle into mature amyloid in the saturation state. The formation of large

globular aggregates and their subsequent disappearance as fibrils grow may explain the earlier observation that Aβ can first form large aggregates that later are converted into small ones.[14]

Because the most toxic Aβ complexes are formed very early in the aggregation process, we speculate that the small aggregates that dominate in the early lag phase either represent the most toxic species or are enriched with the toxic species. It has been proposed that amyloidogenic monomers can aggregate into PFOs and FOs, prior to fibril formation.[7] PFOs are transient intermediates that have to undergo conformational changes, prior to growing into fibrils.[7] It was proposed that monomers may also aggregate to form FOs (fibril nuclei or seeds with the capability of elongating fibrils).[7] Consistent with our observations would be the fact that the most toxic PFOs are associated with the nanoglobules and that the less toxic FOs mainly occur in the larger globular aggregates, where they form nucleation sites for fibrils. However, we do not have evidence from CD spectroscopy that any β structure is forming during the early lag phase (characterized by the most toxic structures); therefore, the nanoglobules and the larger globular aggregates, though they may contain β barrel type structures and fibrillar nuclei, would primarily contain non-β structures. Therefore, it could be that the nanoglobules themselves represent the toxic species and that their fusion into larger aggregates reduces their toxicity, while encouraging their conversion into FOs in a process that marks the start of the transition phase characterized by massive fibril formation.

■ ASSOCIATED CONTENT

S Supporting Information

Figures S1—S6. This material is available free of charge via the Internet at http://pubs.acs.org.

■ AUTHOR INFORMATION

Corresponding Authors

*Department of Biochemistry and Biophysics, Stockholm University, SE-10691 Stockholm, Sweden. E-mail: astrid@dbb.su.se. Fax: +46 (0)8 153 679. Telephone: +46 (0)8 162 444.

*Gorlaeus Laboratory, Leiden Institute of Chemistry, Leiden University, 2300 RA Leiden, The Netherlands. E-mail: abrahams@chem.leidenuniv.nl. Telephone: +31-71-5274213/4557.

Notes

The authors declare no competing financial interest.

■ REFERENCES

(1) Toyama, B. H., Kelly, M. J. S., Gross, J. D., and Weissman, J. S. (2007) The structural basis of yeast prion strain variants. *Nature 449*, 233—237.

(2) Bouchard, M., Zurdo, J., Nettleton, E. J., Dobson, C. M., and Robinson, C. V. (2000) Formation of insulin amyloid fibrils followed by FTIR simultaneously with CD and electron microscopy. *Protein Sci. 9*, 1960—1967.

(3) Greenwald, J., and Riek, R. (2010) Biology of amyloid: Structure, function, and regulation. *Structure 18*, 1244—1260.

(4) Petkova, A. T., Leapman, R. D., Guo, Z., Yau, W.-M., Mattson, M. P., and Tycko, R. (2005) Self-propagating, molecular-level polymorphism in Alzheimer's β-amyloid fibrils. *Science 307*, 262—265.

(5) Hellstrand, E., Boland, B., Walsh, D. M., and Linse, S. (2010) Amyloid β-protein aggregation produces highly reproducible kinetic data and occurs by a two-phase process. *ACS Chem. Neurosci. 1*, 13—18.

(6) Jucker, M., and Walker, L. C. (2013) Self-propagation of pathogenic protein aggregates in neurodegenerative diseases. *Nature 501*, 45—51.

(7) Glabe, C. G. (2008) Structural classification of toxic amyloid oligomers. *J. Biol. Chem. 283*, 29639—29643.

(8) Dobson, C. M. (2003) Protein folding and misfolding. *Nature 426*, 884—890.

(9) Wu, J. W., Breydo, L., Isas, J. M., Lee, J., Kuznetsov, Y. G., Langen, R., and Glabe, C. (2010) Fibrillar oligomers nucleate the oligomerization of monomeric amyloid β but do not seed fibril formation. *J. Biol. Chem. 285*, 6071—6079.

(10) Laganowsky, A., Liu, C., Sawaya, M. R., Whitelegge, J. P., Park, J., Zhao, M., Pensalfini, A., Soriaga, A. B., Landau, M., Teng, P. K., Cascio, D., Glabe, C., and Eisenberg, D. (2012) Atomic view of a toxic amyloid small oligomer. *Science 335*, 1228—1231.

(11) Apostol, M. I., Perry, K., and Surewicz, W. K. (2013) Crystal structure of a human prion protein fragment reveals a motif for oligomer formation. *J. Am. Chem. Soc. 135*, 10202—10205.

(12) Benilova, I., Karran, E., and De Strooper, B. (2012) The toxic Aβ oligomer and Alzheimer's disease: An emperor in need of clothes. *Nat. Neurosci. 15*, 349—357.

(13) Dahlgren, K. N., Manelli, A. M., Stine, W. B., Baker, L. K., Krafft, G. A., and LaDu, M. J. (2002) Oligomeric and fibrillar species of amyloid-β peptides differentially affect neuronal viability. *J. Biol. Chem. 277*, 32046—32053.

(14) Thyberg, P., Tereniusl, L., Tjernbergl, L., Pramanik, A., Bjijrling, S., Thyberg, J., Nordstedtl, C., Berndt, K. D., and Rigler, R. (1999) Amyloid B-peptide polymerization correlation spectroscopy studied using fluorescence. *Chem. Biol. 6*, 53—62.

(15) Luo, J., Otero, J. M., Yu, C.-H., Wärmländer, S. K. T. S., Gräslund, A., Overhand, M., and Abrahams, J. P. (2013) Inhibiting and Reversing Amyloid-β Peptide (1—40) Fibril Formation with Gramicidin S and Engineered Analogues. *Chemistry 19*, 17338—17348.

(16) Luo, J., Yu, C.-H., Yu, H., Borstnar, R., Kamerlin, S. C. L., Gräslund, A., Abrahams, J. P., and Wärmländer, S. K. T. S. (2013) Cellular polyamines promote amyloid-β (Aβ) peptide fibrillation and modulate the aggregation pathways. *ACS Chem. Neurosci. 4*, 454—462.

(17) Luo, J., Mohammed, I., Wa, S. K. T. S., Hiruma, Y., and Abrahams, J. P. (2014) Endogenous Polyamines Reduce the Toxicity of Soluble A β Peptide Aggregates Associated with Alzheimer's Disease. *Biomacromolecules 15*, 1985—1991.

(18) Luo, J., Wärmländer, S. K. T. S., Gräslund, A., and Abrahams, J. P. (2013) Human lysozyme inhibits the in vitro aggregation of Aβ peptides, which in vivo are associated with Alzheimer's disease. *Chem. Commun. 49*, 6507—6509.

(19) Luo, J., Wärmländer, S. K. T. S., Yu, C.-H., Muhammad, K., Gräslund, A., and Pieter Abrahams, J. (2014) The Aβ peptide forms non-amyloid fibrils in the presence of carbon nanotubes. *Nanoscale 6*, 6720—6726.

(20) Wolfe, L. S., Calabrese, M. F., Nath, A., Blaho, D. V., Miranker, A. D., and Xiong, Y. (2010) Protein-induced photophysical changes to the amyloid indicator dye thioflavin T. *Proc. Natl. Acad. Sci. U.S.A. 107*, 16863—16868.

(21) Stroud, J. C., Liu, C., Teng, P. K., and Eisenberg, D. (2012) Toxic fibrillar oligomers of amyloid-β have cross-β structure. *Proc. Natl. Acad. Sci. U.S.A. 109*, 7717—7722.

(22) Gursky, O., and Aleshkov, S. (2000) Temperature-dependent β-sheet formation in β-amyloid Aβ(1—40) peptide in water: Uncoupling β-structure folding from aggregation. *Biochim. Biophys. Acta 1476*, 93—102.

(23) Kusumoto, Y., Lomakin, A., Teplow, D. B., and Benedek, G. B. (1998) Temperature dependence of amyloid β-protein fibrillization. *Proc. Natl. Acad. Sci. U.S.A. 95*, 12277—12282.

(24) Fawzi, N. L., Ying, J., Torchia, D. A., and Clore, G. M. (2010) Kinetics of amyloid β monomer-to-oligomer exchange by NMR relaxation. *J. Am. Chem. Soc. 132*, 9948—9951.

(25) Lee, J., Culyba, E. K., Powers, E. T., and Kelly, J. W. (2011) Amyloid-β forms fibrils by nucleated conformational conversion of oligomers. *Nat. Chem. Biol. 7*, 602—609.

(26) Garai, K., and Frieden, C. (2013) Quantitative analysis of the time course of Aβ oligomerization and subsequent growth steps using tetramethylrhodamine-labeled Aβ. *Proc. Natl. Acad. Sci. U.S.A. 110*, 3321—3326.

(27) Ono, K., Condron, M. M., and Teplow, D. B. (2009) Structure-neurotoxicity relationships of amyloid β-protein oligomers. *Proc. Natl. Acad. Sci. U.S.A. 106*, 14745—14750.

(28) Cremades, N., Cohen, S. I. A., Deas, E., Abramov, A. Y., Chen, A. Y., Orte, A., Sandal, M., Clarke, R. W., Dunne, P., Aprile, F. A., Bertoncini, C. W., Wood, N. W., Knowles, T. P. J., Dobson, C. M., and Klenerman, D. (2012) Direct observation of the interconversion of normal and toxic forms of α-synuclein. *Cell 149*, 1048—1059.

(29) Serio, T. R., Cashikar, A. G., Kowal, A. S., Sawicki, G. J., Moslehi, J. J., Serpell, L., Arnsdorf, M. F., and Lindquist, S. L. (2000) Nucleated Conformational Conversion and the Replication of Conformational Information by a Prion Determinant. *Science 289*, 1317—1321.